

Status of XENON

F. ARNEODO⁽¹⁾, ON BEHALF OF THE XENON COLLABORATION

⁽¹⁾ *New York University Abu Dhabi, United Arab Emirates
(on leave from Laboratori Nazionali del Gran Sasso, INFN, Italy)*

Summary. — XENON is a program for the search of dark matter WIMP particles that has successfully operated two detectors in the Gran Sasso Laboratory, Italy. After the publication, in 2012, of the most stringent limit on spin independent WIMP-nucleus interactions, the XENON100 detector has been taking data, and other analyses have been carried out. At the same time, the new generation detector, XENON1T has been designed and its construction started in 2013.

1. – Introduction

The XENON dark matter program searches for nuclear recoils from WIMPs [1] with liquid xenon detectors. Since the inception of the program, two detectors (XENON10 [2] and XENON100 [3]) have been built and operated underground, at the INFN Laboratori Nazionali del Gran Sasso (LNGS) in Italy [4], to probe WIMP-nucleon scattering cross-sections predicted by SUSY models [5]. A third detector (XENON1T) is presently under construction at the same site. The TPC technology with ultra-pure liquid xenon allows the construction of extremely sensitive detectors that can measure with high accuracy the energy deposition and the spatial coordinates of an interaction in the fiducial volume. Because of the extremely low cross section predicted, and the tiny energy deposition of the recoils, the challenge of XENON, as of any direct detection experiment, is to achieve extremely low background levels and energy threshold. The XENON detectors are two-phase (liquid - gas) time projection chambers (TPCs), with simultaneous detection of the prompt Xe scintillation light at the few keV level, and ionization at the single electron level. The ratio between ionization and scintillation produced by a nuclear recoil (as caused by a WIMP or neutron) is different from that produced by an electromagnetic interaction, allowing a rejection of the majority of the gamma and beta particle background with an efficiency around 99.5% at 50% nuclear recoil acceptance. The event localization with millimeter spatial resolution and the self-shielding capability of the LXe enable further background suppression by selection of a fiducial volume. To demonstrate the XENON detector concept, the R&D phase [6] culminated with a 10 kg scale TPC prototype (XENON10), operated at LNGS from 2006 - 2007 [2], which achieved some of

the best limits on WIMP dark matter. In order to increase the sensitivity to the WIMP-nucleon scattering cross section by more than one order of magnitude, a new TPC with a factor of 10 more mass and a factor of 100 less electromagnetic background was designed to fit inside the improved passive shield built at LNGS for XENON10. That detector, XENON100 was installed at Gran Sasso in 2009. The analysis of 225 days of data taken in 2011 has set the most stringent limit for a very large range of WIMP masses [7]. Only very recently this limit has been superseded by the result of LUX [8]. The performance of XENON100 was accomplished by careful selection of all detector materials regarding intrinsic radioactivity [9], by distilling the xenon target with a dedicated column [3] to keep a low ^{85}Kr contamination, and cleverly designing the detector so that only low radioactive components are close to the target.

2. – Principle of the XENON two-phase TPCs

A schematic of the XENON two-phase (liquid-gas) time projection chamber (TPC) is shown in Fig. 1. A particle interaction in the LXe produces direct scintillation photons and ionization electrons. An electric field is applied across the LXe volume, drifting ionization electrons away from the interaction site. Electrons which reach the liquid - gas interface are extracted into the Xe gas, where the process of proportional scintillation takes place [10]. Both the direct (S1) and the proportional (S2) scintillation light, with 178 nm wavelength, are detected by photomultiplier tubes (PMTs) placed in the liquid (below the cathode) and in the gas phase. The time difference between the S1 and the S2 signals, caused by the finite electron drift velocity in LXe at the given drift field [12] is proportional to the z-coordinate (measured along the drift field direction) of the interaction vertex. The x- and y-coordinates can be inferred from the proportional scintillation hit pattern on the PMTs placed in the gas (top array). Thus, the XENON TPC provides full 3-dimensional vertex reconstruction allowing for the fiducialization of the target to reduce radioactive backgrounds. The different ratio of signals (S2/S1) produced by electronic recoils (from gamma and beta background events) and by nuclear recoils (from WIMPs and neutrons) provides additional background discrimination [13].

3. – The XENON100 detector

A detailed description of the XENON100 detector can be found in [3]. The XENON100 TPC has an almost cylindrical shape of 30.5 cm height and of 15.3 cm radius dividing the 62 kg LXe target (see Fig. 2) from the external veto layer. The walls delineating the cylindrical volume are made of 24 interlocking panels of PTFE (Teflon). The TPC is closed on the bottom by the cathode, and on the top by the gate grid. The gas phase layer is obtained by a diving bell design which allows a precise control of the liquid level, and the same time allowing a 4π coverage of the TPC with the surrounding LXe veto. Two arrays of Hamamatsu R8520-06-Al 1 square PMTs, specially selected for low radioactivity [14], detect the light in the TPC: 80 PMTs are located below the cathode, immersed in the LXe, and they detect the primary S1 signal. 98 PMTs are located above the target in the gas phase, where they detect the S2 signal. A LXe layer of about 4 cm thickness surrounds the TPC on all sides and is observed by additional 64 PMTs of the same type. The TPC is mounted in a double-walled ^{316}Ti stainless steel cryostat, selected for its low activity. Since the radioactive contamination of the cryogenics system, ceramic feedthroughs, etc. cannot be lowered easily, the detector is cooled remotely and all parts with a known high radioactive contamination are installed away from the detector it-

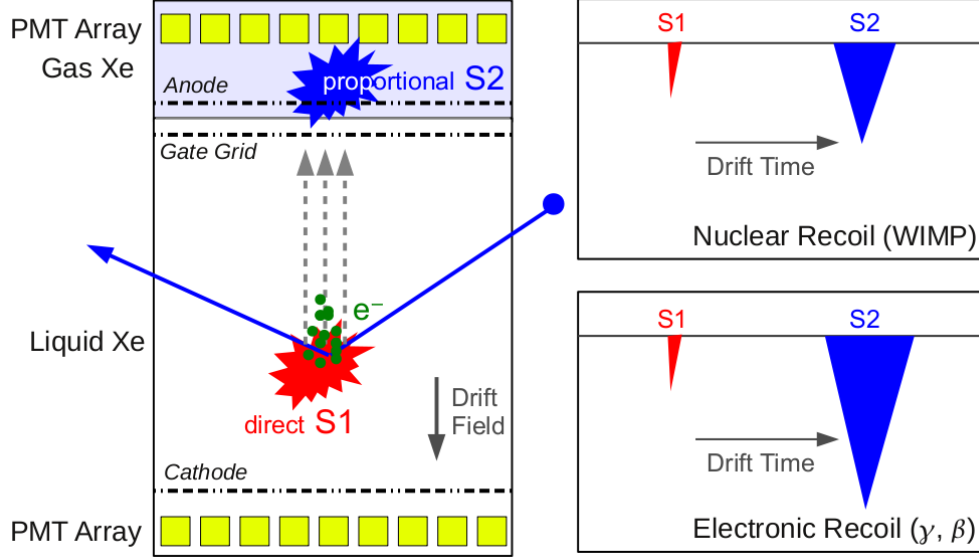


Fig. 1. – (Left) Working principle of the XENON two-phase liquid-gas time projection chamber (TPC). (Right) Sketch of the waveforms of two type of events. The different ratio of the charge (S2) and the light (S1) signal allows for the discrimination between nuclear recoils from WIMPs and neutrons and electronic recoils from gamma- and beta-background.

self, outside the passive shield. The XENON100 experiment is installed underground at LNGS, in the so called "interferometer" tunnel, away from the main experimental halls. Under a rock coverage equivalent to 3100 m of water, the surface muon flux is reduced by a factor 10^6 . In order to reduce the background from the radioactivity of the environment additional passive shielding is needed. A special shield [2] has been designed in collaboration with the Mechanics Service of LNGS, weighting more than 30 t, and composed by 5 cm of OFHC copper, followed by 20 cm of polyethylene, and 20 cm of lead, where the innermost 5 cm consist of lead with a low ^{210}Pb contamination of (26 ± 6) Bq/kg [14]. The entire shield rests on a 25 cm thick slab of polyethylene. An additional outer layer of 20 cm of water or polyethylene has been added on top and on three sides of the shield to reduce the neutron background further. The detector's assembly hangs from the shield door and can be easily accessed without disconnecting pipes or cables.

4. – Recent results

In 2012, the blinded analysis of 225 days of data taking was published [7]. Two candidate events were observed in the nuclear recoil energy range of 6.6 - 30.5 keV_{nr} and in the fiducial volume containing 34 kg of Xe consistent with a background expectation of (1.0 ± 0.2) events. By interpreting this null result in the framework of spin independent WIMP-nucleon interactions, a limit was obtained of $2 \times 10^{-45} \text{ cm}^2$ at 55 GeV and 90% confidence level (see Fig. 3 [7]). That limit has only recently been superseded by the result of LUX [8] as also shown in Fig. 3. As it can be seen, both XENON100 and LUX strong exclusion limits are in contrast with the interpretation, within the same

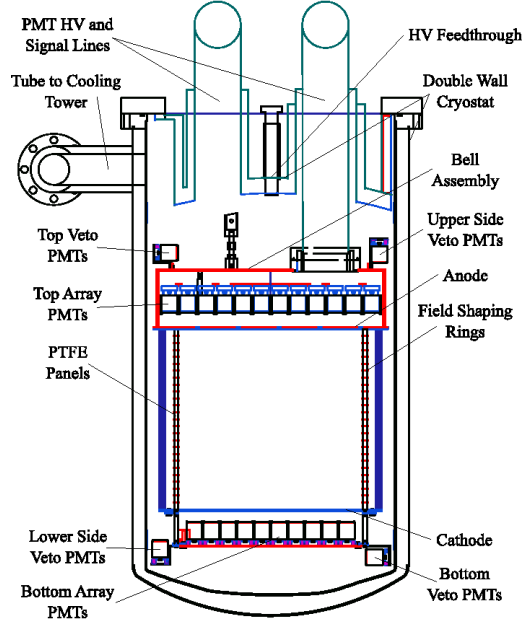


Fig. 2. – Drawing of the XENON100 dark matter detector: the inner TPC contains 62 kg of liquid xenon as target and is surrounded on all sides by an active liquid xenon veto of 99 kg. The diving bell assembly allows for keeping the liquidgas interface at a precise level, while enabling to fill LXe in the vessel to a height above the bell.

interaction model, of possibly positive indications coming from DAMA [16], CRESST [17], and CDMS [18].

Since that publication, the detector has been kept in operation, accumulating more

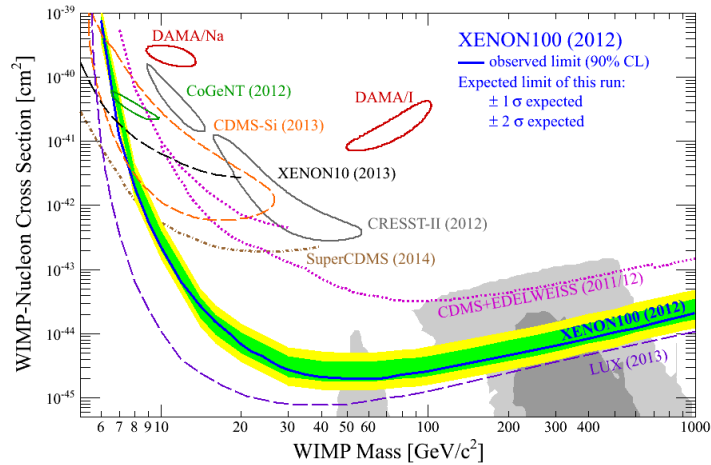


Fig. 3. – Current experimental results on dark matter searches in the framework of WIMP-nucleon spin independent interactions. Adapted from [7].

than 150 days of data that are about to be released with a new paper. In parallel, several analyses have been performed on the already unblinded data. First of all, the data have been interpreted in the framework of spin dependent interactions [19]. In this model, WIMPs couple to the total angular momentum of a nucleus. Nuclei with an odd number of protons and/or neutrons respond to this channel. Xenon is an ideal target, as there are two nonzero spin naturally occurring isotopes ^{129}Xe (spin-1/2) and ^{131}Xe (spin-3/2). In XENON100 their abundances are respectively 26.2% and 21.8%. The XENON100 limits are also here very competitive, especially in the WIMP-neutron cross section where they are presently the most stringent [19].

Another key analysis has been focused on the response of the detector to nuclear recoils, which are the signature of the occurrence of a WIMP scattering. The first problem when dealing with nuclear recoils is to obtain the energy scale, that is the correspondence between the number of photoelectrons (PE) measured and the actual energy of the recoil. For electronic recoils the energy scale is obtained with known γ ray emission lines of calibration sources that are placed close to the detector volume. This allows to infer the correspondence between energy released and photoelectrons in both the S1 and S2 channels. In the case of nuclear recoils, the scintillation light is quenched with respect to electron recoils by a factor called \mathcal{L}_{eff} , which represents the relative scintillation efficiency referred to the 122 KeV line of a ^{57}Co source. In practice, the relation between nuclear recoil energy and the S1 signal is given by the formula [20]:

$$(1) \quad E = \frac{cS_1}{L_y} \frac{1}{\mathcal{L}_{eff}(E)} \frac{S_{ee}}{S_{nr}}$$

where cS_1 represents the S1 signal corrected for any spatially dependent effects, S_{ee} and S_{nr} are the suppression factors of the scintillation light caused by the presence of the electric field, for electron and nuclear recoils respectively.

On the other hand, the relation of the same nuclear recoil energy with the S2 signal is given by:

$$(2) \quad E = \frac{cS2}{Y} \frac{1}{Q_y(E)}$$

where $Q_y(E)$ is the charge yield, that is the number of free electrons per unit energy, while Y is the secondary amplification factor (due to the multiplication in the gas phase), and $cS2$ is the secondary scintillation signal also corrected for spatial effects. The \mathcal{L}_{eff} parameter is crucial in the determination of the energy scale of nuclear recoils, and its uncertainty is the major reason of systematic error in low mass WIMP searches. A measurement of \mathcal{L}_{eff} has been carried out in 2011 [21] with a dedicated setup at the Columbia Astrophysics Laboratory. A further confirmation of the results of that measurement has recently been obtained by a comparison of the response of XENON100 to a $^{241}\text{AmBe}$ neutron source with a detailed Monte Carlo simulation, in which \mathcal{L}_{eff} and Q_y have been left as free parameters. By so doing, the S1 and S2 channels have been assessed independently but simultaneously. The result of the work is a very good agreement of the experimental and simulated spectra of $cS1$ and $cS2$ [20]. Considering this result together with the excellent knowledge of the electromagnetic background [22] of XENON100, and its stability of operation, it may be concluded that the XENON collaboration has a very good control of the systematics of this detector.

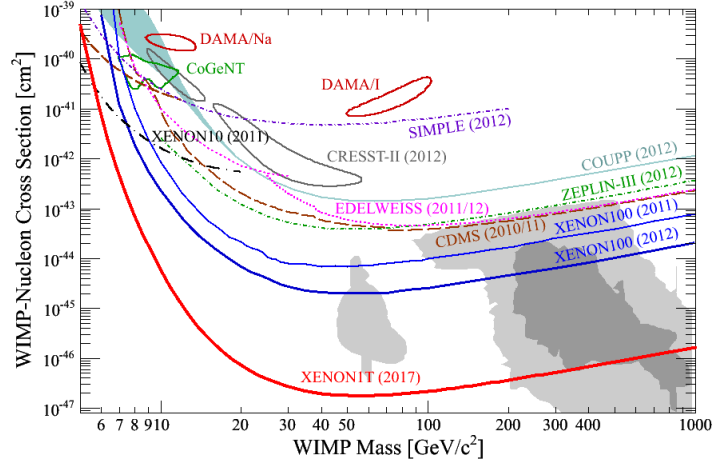


Fig. 4. – The sensitivity reach of XENON1T is shown along current experimental results

5. – The XENON1T detector

With about 3 t of xenon (1 ton fiducial) XENON1T will be the major next step in the search for Dark Matter. The increase in mass is coupled with the reduction in background levels below 6×10^{-5} events/kg/day/keV_{ee}, allowing an improvement factor of 100 in sensitivity with respect to XENON100. In Fig. 4 the sensitivity reach of XENON1T is shown. To stop neutrons from reaching the fiducial volume and to tag cosmic muons (and associated neutrons) the TPC and its cryostat are immersed in 650 t of water contained in a stainless steel tank. The tank is equipped with an active muon veto system with 84 PMTs, allowing a 99% efficiency in tagging crossing muons and 74% efficiency for showering events. The expected neutron background inside the fiducial volume is less than one event per year. A drawing of the complete installation is shown in Fig. 5. The water tank with the cryostat and its support structure are visible on the left. Inside the service building (right), some of the main subsystems of the experiment can be seen: the cryogenics at the top floor, the electronics at the middle level, the gas storage system and the distillation column at the ground level.

The construction of XENON1T is progressing rapidly in the Hall B of the Gran Sasso Laboratory. The first parts constructed are the water tank and the service building. In Fig. 6 a recent image of the interior of the tank is shown. During the summer of 2014 the installation of the other subsystems is foreseen, and the first science run is scheduled in 2015.

REFERENCES

- [1] M.W. Goodman, E. Witten, Phys. Rev. D 31 (1985) 3059.
- [2] E. Aprile et al., XENON10 Collaboration, Astropart. Phys. 34 (2011) 679
- [3] E. Aprile et al., XENON100 Collaboration, Astropart. Phys. 35 (2013) 573
- [4] <http://www.lngs.infn.it>.
- [5] O. Buchmueller et al., Eur. Phys. J. C 71 (2011) 1634.
- [6] E. Aprile et al., Phys. Rev. Lett. 97 (2006) 081302
- [7] E. Aprile et al., Phys. Rev. Lett. 109 (2012) 181301

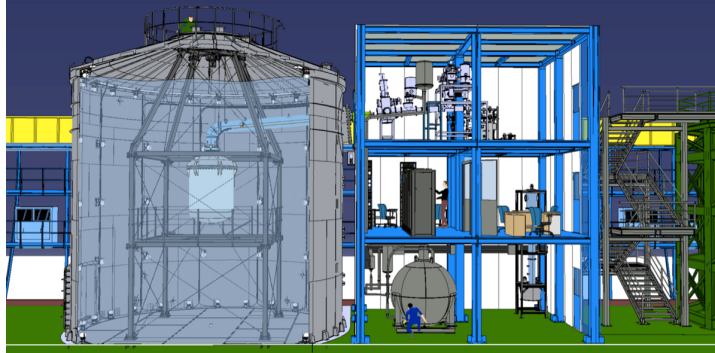


Fig. 5. – Computer generated cross section of the XENON1T installation in Hall B of LNGS as seen from the West side of the Hall.

- [8] LUX Collaboration, Phys. Rev. Lett. 112, 091303.
- [9] E. Aprile et al., XENON100 Collaboration, Astropart. Phys. 35 (2011) 43.
- [10] B.A. Dolgoshein, V.N. Lebedenko, B.U. Rodionov, JETP Lett. 11 (1970) 513.
- [11] E.M. Gushchin et al., Sov. Phys. JETP 45 (1979) 5
- [12] L.S. Miller, S. Howe, W.E. Spear, Phys. Rev. 166 (1968) 871.
- [13] E. Aprile et al., Phys. Rev. Lett. 97 (2006) 081302.
- [14] E. Aprile et al., XENON100 Collaboration, Astropart. Phys. 35 (2011) 43
- [15] E. Aprile et al., XENON100 Collaboration, Phys. Rev. D 83 (2011) 082001.
- [16] R. Bernabei et al., Eur. Phys. J. C **56**, 333-355 (2008).
- [17] G. Angloher et al. (CRESST-II), Eur. Phys. J. C 72, 1971 (2012)
- [18] R. Agnese et al. (CDMS-II Collaboration) Phys. Rev. Lett. 111, 251301 (2013).
- [19] E. Aprile et al., Phys. Rev. Lett. 111 (2013) 021301
- [20] Phys. Rev. D **88**, 012006 (2013).

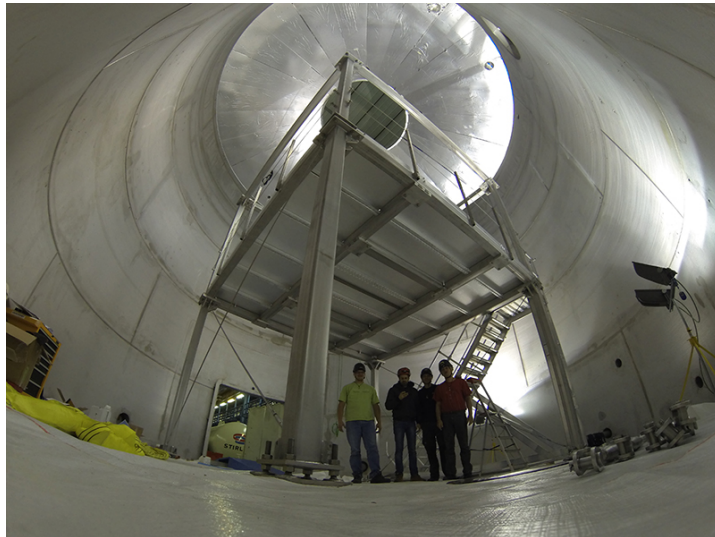


Fig. 6. – The interior of the water tank with the cryostat support structure, May 2014

- [21] Phys. Rev. C **84**, 045805 (2011).
- [22] Phys. Rev. D **84**, 082001 (2011).